Int. J. Multiphase Flow, Vol. 4, pp. 413–425. Pergamon/Elsevier, 1978. Printed in Great Britain

HEAT TRANSFER TO NON-NEWTONIAN LAMINAR FALLING LIQUID FILMS WITH SMOOTH WAVE FREE GAS–LIQUID INTERFACE

V. NARAYANA MURTHY† and P. K. SARMA
Department of Mechanical Engineering, Andhra University, Visakhapatnam-530 003, India

(Received 15 February 1977)

Abstract—The present paper investigates analytically the problem of heat transfer to a non-Newtonian laminar falling liquid film flowing along an inclined wall for the thermally developing and thermally developed regions. In the developing region of the temperature profile, the Nusselt number decreases monotonically until the thermal boundary layer touches the interface. But immediately after this point, the liquid film thickness decreases as well as the temperature difference in the film. The influence of parameters such as α (i.e. Fr/Re_{mod} ratio), γ (i.e. modified form of $\rho\mu$), modified Prandtl number and the flow behaviour index 'n' on heat transfer results is also presented.

INTRODUCTION

In many industrial applications, heating or cooling of liquids is achieved by allowing the liquid to flow in the form of a thin film along a solid boundary maintained at a different temperature from that of the bulk. Fulford (1964) presented an excellent review on falling liquid films both for laminar and turbulent flow conditions of the film. Modifying Dukler & Bergelin (1952) analysis, Hewitt (1961) investigated analytically co-current upward annular turbulent flow phenomena of liquid films. Assuming that the gas phase does not give rise to any shear stress at the free surface, Astarita *et al.* (1964) measured experimentally the liquid film thickness as a function of inclination of the solid boundary and the discharge rate of the fluids whose rheological properties were not given. Normand *et al.* (1970) studied analytically the laminar liquid film thicknesses using the power law model for shear deformation. Their analysis also excludes the possible effects of interfacial drag of the quiescent gas. Sylvester *et al.* (1973) have presented both analytical and experimental investigations pertaining to non-Newtonian falling liquid films assuming the interface to be wavy and the flow is fully developed. Murty & Sastry (1973) studied analytically the problem of accelerating falling liquid films of the Newtonian type by taking into account the interfacial drag and thus their analysis is an improvement over other investigators. Recently an analytical expression was proposed in closed form by Stücheli & Özisik (1976) for the determination of hydrodynamic entrance length for liminar falling liquid films. However, the analysis is mainly confined to Newtonian fluids and the influence of interfacial shear is not accounted for. Narayana Murthy & Sarma (1977) obtained entrance lengths of laminar, accelerating non-Newtonian falling liquid films for no drag condition at the vapor–liquid interface. In a recent article, Narayana Murthy & Sarma (1978) further improved the analysis by including the interfacial drag at the vapor–liquid interface due to the presence of quiescent gas adjacent to liquid film. It was observed that for certain values of α (i.e. Fr/Re_{mod}), the change in the curvature of the free surface is very rapid and under such circumstances the surface tension forces undoubtedly play significant role in the dynamics of the liquid films. However, the results of the analysis by Narayana Murthy & Sarma (1978) pertaining to the mean thickness of the liquid films for $0.4 \leq n \leq 1.4$ are in confirmity with the experimental observations of Sylvester *et al.* (1973).

In the present article, the problem of heat transfer to the thin, non-Newtonian falling liquid films is considered for the thermally developing and developed regions.

†Current address: Higher Petroleum Institute, Tobruk, Libya.

PHYSICAL MODEL

The liquid at an initial temperature t_o is made to flow at constant steady discharge rate from a slit whose height $h_o \ll L$, where L is the characteristic length of the plate. The plate is maintained at isothermal conditions t_w and $t_w > t_o$ for $x \geq 0$. The physical configuration of the model is shown in figure 1. In the present analysis, the gas–liquid interface is assumed wave free and smooth. Such a condition is possible for certain range of α (i.e. Fr/Re_{mod}) as observed from the results of Narayana Murthy & Sarma (1978). Further, Sylvester *et al.* (1973) concluded that for Re less than the critical value Re_c, the interface is smooth and also when $Re > Re_c$, the visual observations confirmed that the onset of ripples or waves occured only at distances away from the exit of the slit. The present article confines only to the case of wave free non-Newtonian accelerating falling films. The moving liquid film sets the adjacent gas to motion and the effect of interfacial drag due to the presence of the gas on the thickness of the liquid film is found to be minimal.

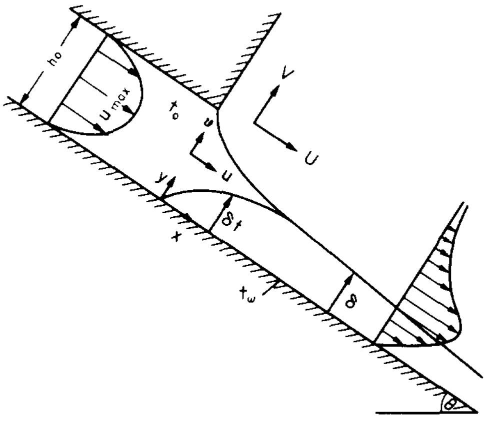

Figure 1. Physical configuration.

ANALYSIS

The equations of conservation of mass, momentum and energy are respectively as follows: For the liquid region,

$$\frac{\partial u}{\partial x} + \frac{\partial v}{\partial y} = 0, \qquad [1]$$

$$\rho\left(u\frac{\partial u}{\partial x} + v\frac{\partial u}{\partial y}\right) = \frac{\partial \tau}{\partial y} + g(\rho - \rho_g)\sin\theta, \qquad [2]$$

$$u\frac{\partial t}{\partial x} + v\frac{\partial t}{\partial y} = \beta\frac{\partial^2 t}{\partial y^2} \qquad [3]$$

where u, v are the liquid velocity components in x- and y-directions respectively; ρ is the density of liquid and ρ_g that of the gas; τ is the shear stress; β is the thermal diffusivity; g is the acceleration due to gravity and θ is the angle of inclination to the horizontal.

The boundary conditions for the equation of motion are

$$u = v = 0 \quad \text{at} \quad y = 0, \qquad [4]$$

$$u = 4u_{max}[(y/h_o) - (y^2/h_o^2)] \quad \text{at} \quad x = 0, \qquad [5]$$

where

$$u_{max} = 3G/2\rho h_o \qquad [6]$$

and G is the mass flow rate per unit width.

Likewise, the boundary conditions for the conservation of energy equation are as follows:

$$\text{at } x = 0 \quad t = t_o \quad (\text{for } 0 < y \leqslant h_o), \tag{7}$$

$$\text{at } y = 0 \quad t = t_w \quad (\text{for } x \geqslant 0). \tag{8}$$

In addition, the conservation of mass and momentum equations in the gas phase adjacent to the liquid film are

$$(\partial U/\partial x) + (\partial V/\partial Y) = 0, \tag{9}$$

$$\rho_g\left(U\frac{\partial U}{\partial x} + V\frac{\partial U}{\partial Y}\right) = \mu_g\frac{\partial^2 v}{\partial y^2} \tag{10}$$

where U and V are the gas velocity components; Y is the ordinate normal to the surface of the plate and measured from the gas–liquid interface; and μ_g is dynamic viscosity of the gas.

The boundary conditions for the equations of the gas phase are

$$U = U_i \text{ (interfacial velocity) at } y = \delta, \tag{11}$$

$$V = 0 \text{ (no phase transformation) at } y = \delta, \tag{12}$$

where δ is local liquid film thickness.

For the gas–liquid systems at $x > 0$ by an order of magnitude analysis it can be shown that $(\Delta/\delta) \sim \sqrt{(\nu_g/\nu_L)}$ for $n = 1$ (Δ being local gas film thickness and ν kinematic viscosity). Thus, it is very suggestive that $\Delta/\delta \gg 1$ for $x > 0$. Bearing this particular aspect in mind and also the absence of phase transformation at gas–liquid interface, [9] and [10] are transformed into integral form as below. It is true

$$\mu(\partial u/\partial y)^n|_{y=\delta} = \mu_g(\partial U/\partial Y)|_{Y=0} \tag{13}$$

where μ = the index of consistency (and becomes Newtonian viscosity for $n = 1$); n is the flow behaviour index and $n < 1$ represents pseudoplastic fluids, $n > 1$ represents dilatant fluids, and $n = 1$ represents Newtonian fluids.

Equation [13] is the equal shear condition at the gas–liquid interface. Thus, [1]–[13] describe the problem mathematically to obtain both velocity and temperature profiles. In order to facilitate solution, [1]–[3], [9] and [10] are put in an integro-differential form as follows:

For the liquid region,

$$\frac{\mathrm{d}}{\mathrm{d}x}\int_o^\delta \rho u \,\mathrm{d}y = 0, \tag{14}$$

$$\frac{\mathrm{d}}{\mathrm{d}x}\int_o^\delta \rho u^2 \,\mathrm{d}y = (\tau_{iL} - \tau_w) + g\rho\delta\sin\theta. \tag{15}$$

For the gas region,

$$\frac{\mathrm{d}}{\mathrm{d}x}\int_o^\Delta \rho_g U \,\mathrm{d}Y = -\rho_g V_\Delta, \tag{16}$$

$$\frac{\mathrm{d}}{\mathrm{d}x}\int_o^\Delta \rho_g U^2 \,\mathrm{d}Y = -\tau_{ig} \tag{17}$$

where the subscript iL represents interface liquid, ig represents interface gas and Δ at Δ.

In the liquid region, the energy equation takes the shape

$$\frac{d}{dx}\int_o^{\delta_t} \rho u C_p(t-t_o)\,dy = -K\left.\frac{dt}{dy}\right|_{y=0} \quad [18]$$

where C_p is specific heat of liquid at constant pressure, K is thermal conductivity of the liquid and δ_t is thermal boundary layer thickness.

In [18] the upper limit of the integral is δ_t, the thermal boundary layer which is smaller than the actual thickness of the liquid film in the region $x = 0$. The thermal boundary layer, δ_t starts developing from a value $\delta_t = 0$ at $x = 0$ to $\delta_t = \delta$ at some unknown location, x. This particular region can be termed as the thermally developing region. Beyond this point, the interface temperature also changes in such a manner that the energy balance is satisfied. In the thermally developed region, the energy equation in integro-differential form can be written as

$$\frac{d}{dx}\int_o^{\delta} \rho u C_p t\,dy = -K\left.\frac{\partial t}{\partial y}\right|_{y=0}. \quad [19]$$

Thus, [15]–[19] can be solved only when the velocity and temperature profiles are known *a priori*. The following are the velocity profiles assumed in the analysis both in the liquid and gas phases. For the liquid region,

$$u = 4u_{\max}f_1\left(\frac{f_2+2}{3}\eta - \eta^2\right) \quad [20]$$

where η, the dimensionless space coordinate $= y/\delta$ and f_1 and f_2 are unknown functions of x. The velocity profile in the gas phase should satisfy the following conditions, viz.,

$$U = U_i \quad \text{at } Y = 0, \quad [21]$$

$$\frac{\partial U}{\partial Y} = \frac{\partial^2 U}{\partial Y^2} = \cdots\cdots = \frac{\partial^m U}{\partial Y^m} = 0 \quad \text{at } Y = \Delta \quad [22]$$

where m is an arbitrary integer representing the order of the derivative. Equation [22] can be construed as a smoothen constraint at $Y = \Delta$. It is observed by Narayana Murthy & Sarma (1978) that the choice of a fourth degree polynomial as a velocity profile gave identically same values as observed by Murty & Sastry (1973). However, Murty & Sastry (1973) used an exponential function for the gas phase velocity. Thus, for further analysis the following velocity profile is chosen:

$$\frac{U}{U_i} = \left(1 - \frac{Y}{\Delta}\right)^4. \quad [23]$$

The temperature profile for the thermally developing region is

$$\frac{t-t_o}{t_w-t_o} = \bar{\theta} = 1 - \frac{3}{2}\frac{u}{\delta_t} + \frac{1}{2}\left(\frac{y}{\delta_t}\right)^3, \quad [24]$$

satisfying the conditions

$$t = t_o \quad \text{at } y = \delta_t, \quad [25]$$

$$t = t_w \quad \text{at } y = 0, \quad [26]$$

$$\partial t/\partial y = 0 \quad \text{at } y = \delta_t, \quad [27]$$

$$\partial^2 t/\partial y^2 = 0 \quad \text{at } y = 0. \quad [28]$$

For the thermally developed region,

$$\frac{t-t_o}{t_w-t_o}=\bar{\theta}=1-\phi(x)\left[\frac{3}{2}\frac{y}{\delta}-\frac{1}{2}\left(\frac{y}{\delta}\right)^3\right] \quad [29]$$

where $\phi(x)$ is unknown function of x (i.e. flow direction). At the point of transition between the thermally developing region and thermally developed region, the temperature profiles, (i.e. [24] and [29]) should be identical. In other words, $\phi(x)=1$ at $x=x_{\text{critical}}$. Thus, [15], [17]–[19] can be manipulated respectively to the forms shown below:

$$\frac{d}{d\lambda}[f_1\{10f_2+(4/f_2)-5\}]=\frac{135}{8}\left[\frac{1}{\alpha f_1 f_2}-(4/3)^n f_1^{2n} f_2^n\{(4-f_2)^n+(f_2+2)^n\}\right], \quad [30]$$

$$\frac{d}{d\lambda}\left[\frac{f_1^{(3-2n)}(f_2-1)^3}{\{f_2(4-f_2)\}^n}\right]=\left(\frac{4^{2n-4}}{3^{2n-5}}\right)\gamma[f_1^2 f_2(4-f_2)]^n, \quad [31]$$

$$\frac{d}{d\lambda}\left[\frac{1}{f_2}\left\{\frac{(f_2+2)\zeta^2}{6}-\frac{5\zeta^3}{24}\right\}\right]=\frac{15}{8}\frac{f_1 f_2}{\zeta}\frac{1}{Pr^*}, \quad [32]$$

$$\frac{d}{d\lambda}\left[\frac{1}{f_2}\left\{\left(\frac{f_2+2}{6}\right)\left(1-\frac{4\phi}{5}\right)+\frac{7\phi}{24}-\frac{1}{3}\right\}\right]=\frac{3}{8}\left(\frac{f_1 f_2 \phi}{Pr^*}\right), \quad [33]$$

where λ, dimensionless distance $=(\mu u_{\max}^{n-2}x/\rho h_o^{n+1})$; α, dimensionless number $=Fr/Re_{\text{mod}}$; Fr, Froude number $=(u_{\max}^2/gh_o \sin\theta)$; Re_{mod}, modified Reynolds number $=(\rho u_{\max}^{2-n}h_o^n/\mu)$; γ, dimensionless number $=(\mu\rho u_{\max}^{n-1}/\mu_g\rho_g h_o^{n-1})$; ζ, dimensionless ratio $=\delta_t/\delta$; and Pr^*, modified Prandtl number $=(\mu C_p/K)(u_{\max}^{n-1}/h_o^{n-1})$.

The boundary conditions for [30] to [33] are

$$\text{at } \lambda=0 \quad f_1=f_2=1 \text{ and } \zeta=0,$$

$$\text{at } \lambda=\lambda_{\text{critical}}(\text{unknown}), \quad \phi=1.$$

Equations [30] to [32] can be solved simultaneously for various values of λ till such time ζ tends to 1. However, when $\zeta=1$, the simultaneous solution is accomplished with [30], [31] and [33] to obtain the unknowns f_1, f_2, ζ and ϕ. No further attempt is made to analyse the dynamics of the liquid film, as the problem is already presented by the authors elsewhere (Narayana Murthy & Sarma, 1978). To conserve space, the heat transfer aspects only are discussed further.

HEAT TRANSFER COEFFICIENT

From a practical point of view, the heat-transfer coefficient is important and by definition we have

$$q_w=-K(\partial t/\partial y)|_{y=0}. \quad [34]$$

Also we tentatively define the heat-transfer coefficient taking the inlet temperature as reference value,

$$q_w=h(t_w-t_o) \quad [35]$$

where h is the local heat-transfer coefficient.

Thus, from [24], [34] and [35] for the thermally developing region we get

$$hh_o/K=Nu_1(\text{Nusselt number})=(3/2)(f_1 f_2/\zeta). \quad [36]$$

For the thermally developed region from [29], [34] and [35] we get the local Nusselt value as

$$hh_o/K = Nu_2 = 1.5\phi f_1 f_2. \qquad [37]$$

RESULTS

Temperature profiles

The temperature profiles at various locations for different values of 'n' and for two values of α are shown plotted in figures 2 and 3. It is observed that for $\alpha = 0.01$ and $\lambda = 0.001$ the temperature profile is unique and more or less identical for all values of 'n' ($0.4 < n < 1.4$). For

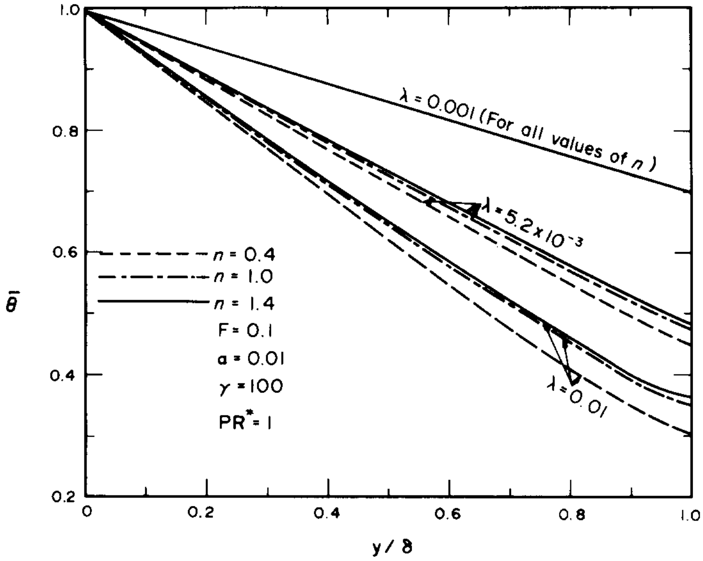

Figure 2. Temperature profiles at different locations.

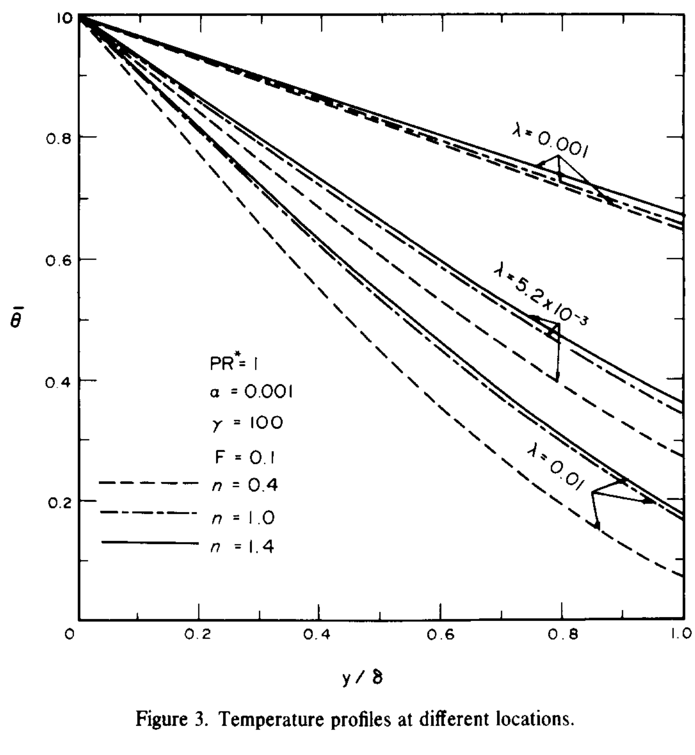

Figure 3. Temperature profiles at different locations.

$\alpha = 0.001$ and $\lambda = 0.001$, separate temperature profiles are observed for different values of 'n'. However, in all the cases at distances far away from the slit (i.e. $\lambda > 0.001$), the distortion from the linearity in the temperature profiles is more pronounced. Further, for the given location, the slope of the temperature curve is dependent on 'n', the index in the Ostwald-de-Waele expression. As 'n' decreases, the gradient in the temperature profile at the wall decreases.

The influence of γ on the temperature profiles for different values of the index 'n' is shown in figure 4. For $n < 1$, as γ increases, the slope of the temperature function at the solid boundary increases. However, for $n \geq 1$, the reverse is the case. Further, the effect of F on the temperature profiles is not observed and totally absent as evident from figure 4 [where F is defined by the authors in Reference (1978)].

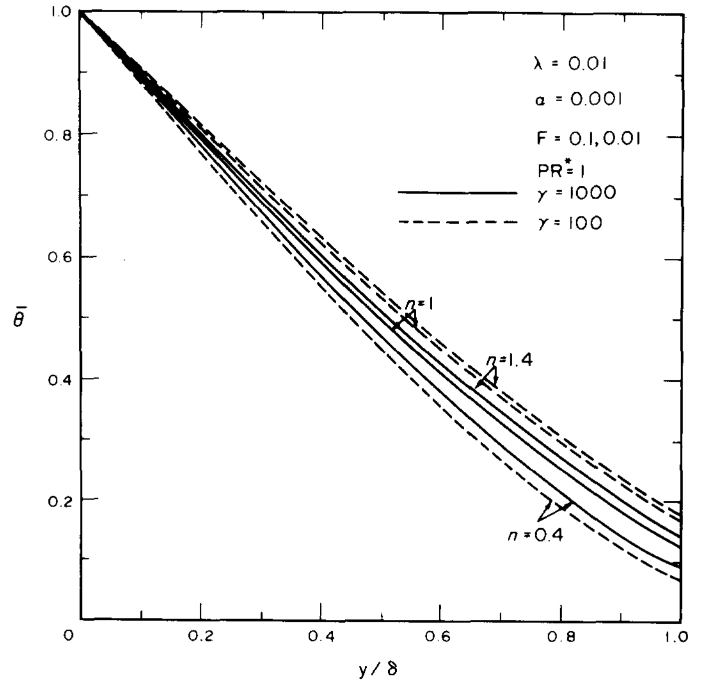

Figure 4. Influence of γ on temperature profiles.

The influence of α on temperature profiles at $\lambda = 0.01$ is shown for two values of α (i.e. $\alpha = 0.001, 0.01$) in figure 5 for different values of 'n'. It is observed that the profiles for $\alpha = 0.01$ lie above the profiles for $\alpha = 0.001$.

The influence of the modified Prandtl number on the temperature profiles in the thermally developing and thermally developed regions is respectively shown in figures 6 and 7. As Prandtl number increases for a given value of 'n', the gradient of the temperature curve decreases in the thermally developing region. However, a different trend is observed in the thermally developed region. For Prandtl number 10 and for a given value of 'n', the slope of the temperature profile is more than that for the case of Prandtl number 5. Thus, the nature of the temperature profiles are different for the two regions (thermally developing and thermally developed regions).

Heat transfer results

The heat transfer results are shown plotted in figures 8–15. In the thermally developing region, the influence of the modified Prandtl number is shown in figure 8 for very low values of λ (i.e. $\lambda < 24 \times 10^{-7}$). The heat-transfer curves are monotonic in nature and as can be anticipated, at $x = 0$, the Nusselt number is maximum and gradually goes on decreasing along the flow direction. As one would expect, increase in modified Prandtl number leads to an increase in the local Nusselt value. Further, one interesting feature is that for low values of λ (i.e.

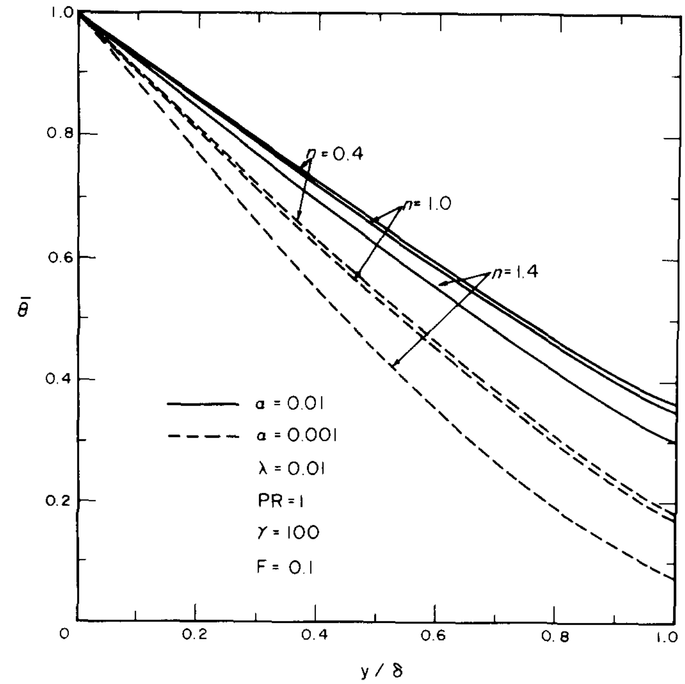

Figure 5. Influence of α on temperature profiles.

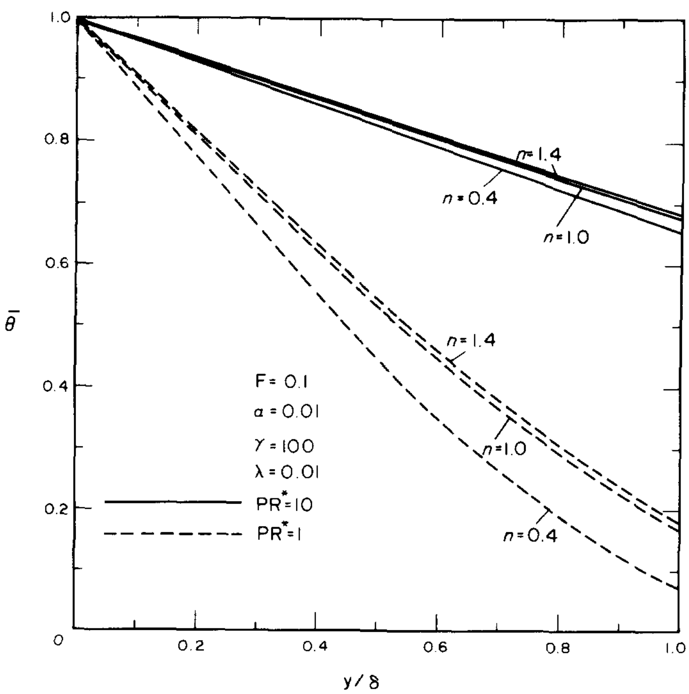

Figure 6. Influence of Pr^* on temperature profiles.

$\lambda < 24 \times 10^{-7}$), the influence of '$n$' on hat-transfer results is not observed and a single heat transfer characteristic is obtained for different values of 'n' (i.e. $0.4 < n < 1.4$) for that particular combination of the parameters F, α and γ.

For very high values of λ (i.e. $0.005 \leq \lambda \leq 0.12$), the variation of Nusselt number along the flow direction is shown in figures 9 and 10 for modified Prandtl number values of 5 and 100. In

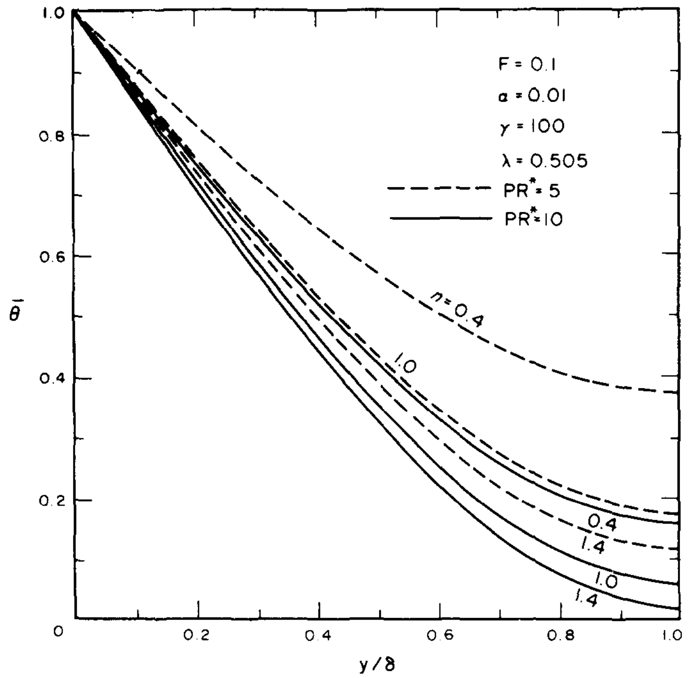

Figure 7. Influence of Pr^* on temperature profiles (thermally developed region).

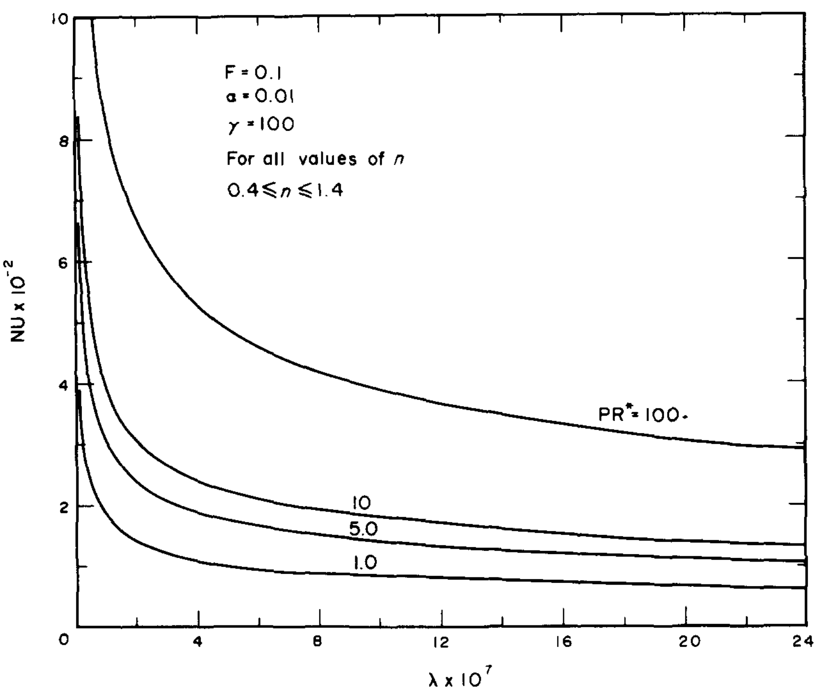

Figure 8. Influence of Pr^* on Nu for $\lambda < 24 \times 10^{-7}$.

both the cases at distances far away from the exit of the slit, it is observed that for pseudoplastic fluids, the Nusselt values are more than those for Newtonian and dilatant fluids.

In the developing region, the influence of γ on the heat transfer variation along the flow direction is shown in figure 11. As γ increases, the transfer coefficient increases.

From figure 12, it is clear that as α increases, the Nusselt number decreases. In addition, for $\alpha = 0.1$ different curves are obtained for different values of 'n' but whereas for low values of α

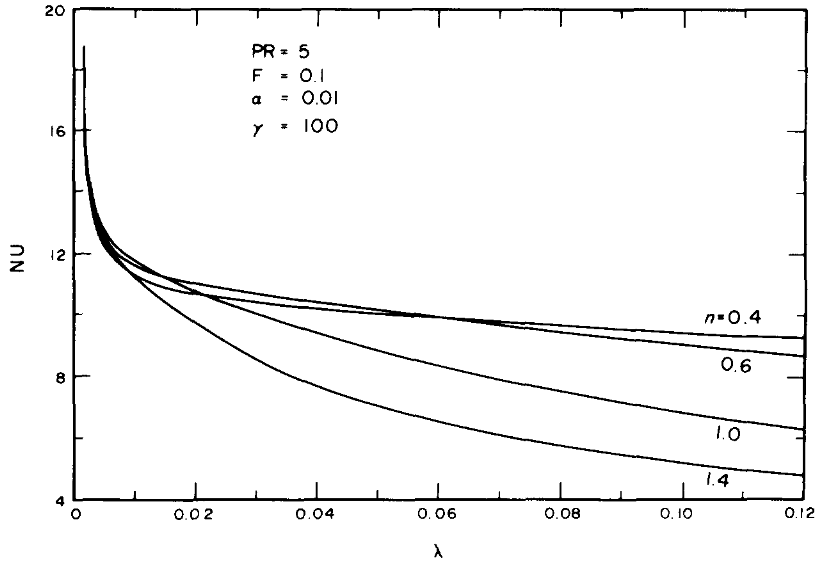

Figure 9. Influence of 'n' on Nu for $0.005 \leq \lambda \leq 0.12$.

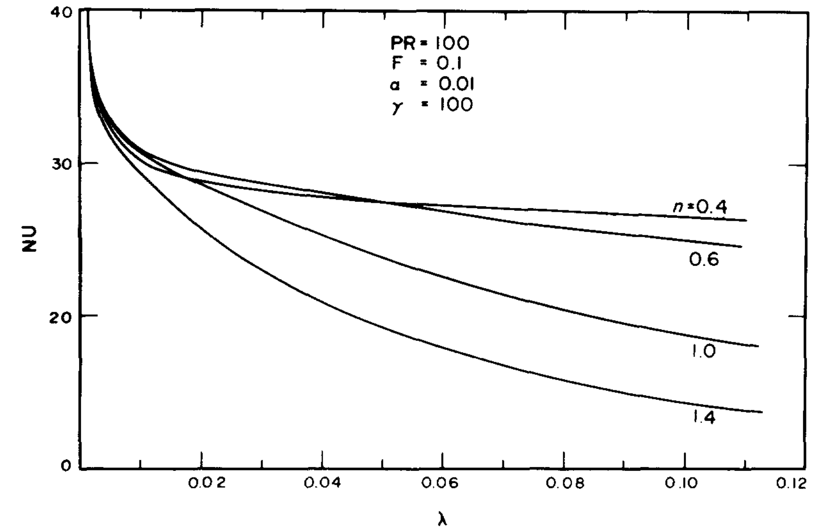

Figure 10. Influence of 'n' on Nu for $0.005 \leq \lambda \leq 0.12$.

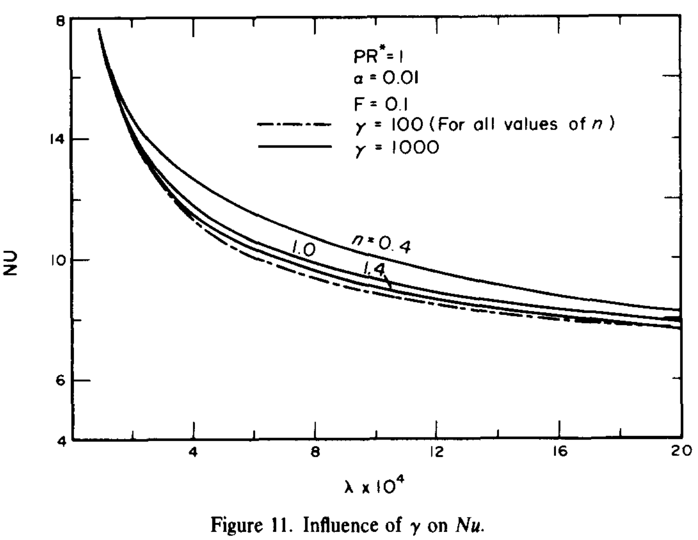

Figure 11. Influence of γ on Nu.

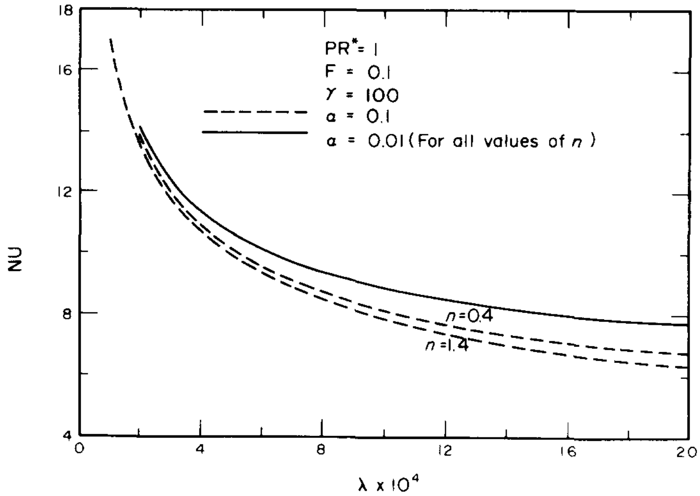

Figure 12. Influence of α on Nu.

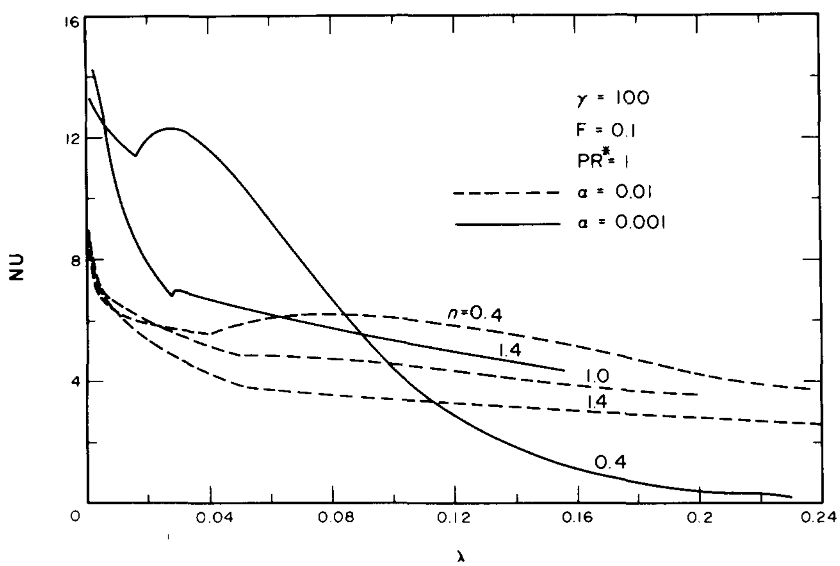

Figure 13. Influence of α on Nu (for both regions).

(i.e. $\alpha = 0.01$), the effect of 'n' on the heat transfer characteristics is not being felt, i.e. a single monotonic characteristic is obtained.

In figures 13 and 14 the influence of α on the heat-transfer results is shown. As already pointed out, the Nusselt number monotonically decreases in the developing region and when the thermal boundary layer attains the same thickness as the liquid film, a slight increase in heat transfer values for $\alpha = 0.001$ and 0.01 is observed. The decrease in the local Nusselt number in the thermally developing region is because of the monotonic increase in the thickness of the thermal boundary layer. The thermal boundary layer lies between two isotherms, viz. the constant wall temperature and the constant inlet temperature. Immediately after the developing thermal boundary layer meets the interface, the interface is no longer an isotherm and the interface temperature increases. Thus, the Nusselt variation depends on the rate at which interface temperature is increasing as well as on the rate at which the liquid film thickness is decreasing (see [37]). From figures 13 and 14 it is also seen that for small values of α the Nusselt number falls very steeply to a small value whereas for large values of α the rate of decrease is slower. Small values of α means smaller film thicknesses which in turn are

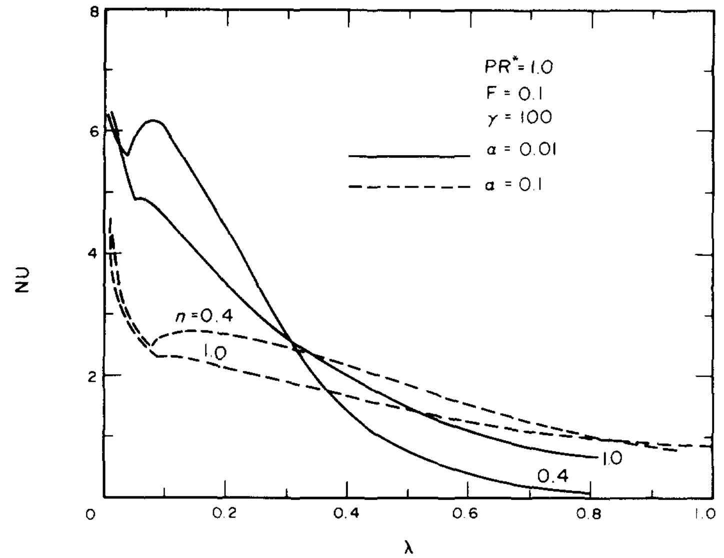

Figure 14. Influence of α on Nu (for both regions, i.e. $\lambda < 1.0$).

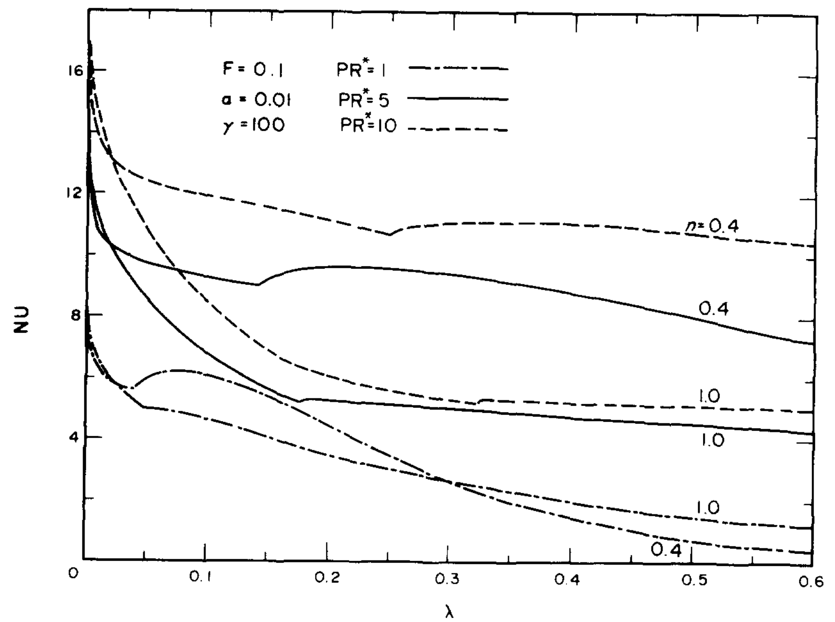

Figure 15. Influence of Pr^* on Nu.

responsible for heating to be affected at a faster rate. The influence of 'n' on Nusselt number is also shown in figure 14. In the thermally developed region for $\lambda > 0.9$, as 'n' increases the Nusselt value also increases.

In figure 15 the influence of modified Prandtl on heat transfer results is shown. It is observed that in the fully developed thermal region and for $\lambda > 0.3$ as Prandtl number decreases, the Nusselt number increases. However, all the computations are limited to $\lambda \leq 1.0$.

Acknowledgements—The authors thank the reviewers for their constructive comments.

REFERENCES

ASTARITA, G., MARRUCCI, G. & PALUMBO, G. 1964 Non-Newtonian gravity flow along inclined plane surfaces. *I/EC Fundamentals* 3, 333–339.

BRULEY, D. F. 1965 Predicting vertical film flow characteristics in the entrance region. *A.I.Ch.E.Jl* **11**, 945–950.

CERRO, R. L. & WHITAKER, S. 1971 Entrance region flows with a free surface: The falling liquid films. *Chem. Engng Sci.* **26**, 785–798.

DUKLER, A. E. & BERGELIN, O. P. 1952 Characteristics of flow in falling liquid films. *Chem. Engng Prog.* **48**, 557–563.

FULFORD, G. D. 1964 The flow of liquids in thin films. *Advances in Chemical Engineering*, Vol. 5, pp. 151–236. Academic Press, New York.

HASSAN, N. A. 1967 Laminar flow along a vertical wall. *J. Appl. Mech.* **34**, 535–537.

HAUGEN, R. 1968 Laminar flow along vertical wall. *J. Appl. Mech.* **35**, 631–633.

HEWITT, G. F. 1961 Analysis of annular two-phase flow: Application of the Dukler Analysis to vertical upward flow in a tube. AERE Report No. R-3680.

MURTY, N. S. & SASTRY, V. M. K. 1973 Accelerating laminar liquid film along an inclined wall. *Chem. Engng Sci.* **28**, 869–874.

NARAYANA MURTHY, V. & SARMA, P. K. 1977 A note on hydrodynamic entrance lengths of non-Newtonian laminar falling liquid films. *Chem. Engng Sci.* **32**, 566–567.

NARAYANA MURTHY, V. & SARMA, P. K. 1978 Dynamics of developing laminar non-Newtonian falling liquid films with free surface. *J. Appl. Mech.* **45**, 19–25.

NORMAND, T., BERNARD, C. & CORNEILLE, J. L. 1970Vérification expérimentale de l'epaisseur du film pour des liquids non-Newtonians s'écaulant par gravité, sur un plan incline. *Can. J. Chem. Engng* **48**, 17–26.

STÜCHELI, A. & ÖZISIK, M. N. 1976 Hydrodynamic entrance lengths of laminar falling films. *Chem. Engng Sci.* **31**, 369–372.

SYLVESTER, N. D., TYLER, J. S. & SKELLAND, A. H. P. 1973 Non-Newtonian thin films: theory and experiment. *Can. J. Chem. Engng* **51**, 418–429.